J Braz. Soc. Mech. Sci. Eng.
DOI 10.1007/s40430-016-0558-y

TECHNICAL PAPER

Design and structural optimisation of a tractor mounted telescopic boom crane

H. Kursat Celik[1] · Allan E. W. Rennie[2] · Ibrahim Akinci[1]

Received: 13 March 2015 / Accepted: 8 April 2016

Abstract In this research, an application algorithm, which can be used in computer-aided design/engineering (CAD/CAE) and structural optimisation-based design studies of agricultural machineries, is introduced. This developed algorithm has been put in practice in a case study for a tractor mounted telescopic boom crane. The algorithm consists of both numerical and experimental methods and it includes material testing, three-dimensional (3D) computer-aided design and finite-element method (FEM)-based analysis procedures, structural optimisation strategy, physical prototyping, physical testing and design validation procedures. Following the visual and physical validation procedures carried out in the case study, the crane's physical prototype was manufactured and the optimised design was approved for ongoing production. The study provides a unique CAD/CAE and experimentally driven total design pathway for similar products, which contributes to further research into the utilisation of engineering simulation technology for agricultural machinery design, analysis and related manufacturing subjects.

Keywords Agricultural machinery design · Computer-aided design · Computer-aided engineering · Structural optimisation

Technical Editor: Fernando Antonio Forcellini.

✉ H. Kursat Celik
hkcelik@akdeniz.edu.tr

1 Department of Agricultural Machinery and Tech.' Faculty of Agriculture, Eng., Akdeniz Uni. Antalya, Antalya, Turkey

2 Lancaster Product Development Unit, Department of Engineering, Lancaster Uni., Lancaster, UK

1 Introduction

According to the US Accreditation Board of Engineering and Technology, 'Engineering Design' is the process of devising a system, component, or process to meet desired needs. It is a decision-making process (often iterative), in which the basic science, mathematics and engineering sciences are applied to convert resources optimally to meet a stated objective [1, 2]. In other words, design is to create a new product that turns into profit and benefits society in some way. However, design is a sum of the specific processes, whose steps can be customised depending on the design objectives and the product. It comprises common main phases which are needs assessment, problem formulation, abstraction and synthesis, analysis and implementation. In fact, in a conventional design progression, often, designers have to repeat the same steps many times, which is why designing is described as highly iterative in nature [3]. In this context, the implementation of CAD/CAE technologies helps to shorten this repetition of the steps and aids in increasing efficiency in the product design process [4]. Mechanical design engineering has been improving through the application of CAD/CAE applications, since the 1950s [5]. There is no doubt that a CAD/CAE driven product design strategy can provide benefits in the design of agricultural tools and machinery systems [6], and it is true to say that, relatively, the agricultural machinery design and manufacturing industry in Turkey have not fully embraced exploitation of this advanced technology. In Turkey, the majority of the agricultural machinery manufacturers that provide machinery support for agricultural production are in the small- and medium-sized enterprises classification of companies. To move them to today's competitive global market, it is an inevitable process for a better agricultural production and from an industrial development perspective.

To enable this, some key paths can be introduced, including knowledge support to equip them with current advanced CAD and manufacturing driven technology and the necessary strategy for utilisation. As such, this research describes a unique application algorithm in an industrially focussed and applied case study for a sample tractor mounted lifting mechanism and for the agricultural enterprises.

Nowadays, it is possible to employ a variety of large capacity tools and machinery, designed for lifting, loading and transportation operations in different sectors of industry. However, such machinery may not be suitable for small- and medium-sized agricultural enterprises due to important limitations, such as high purchase cost, and large capacity and size which are not preferred by small- and medium-sized growers, professional operator needs, etc. Therefore, most of the small- and medium-sized growers prefer to use lower capacity, more simplistic lifting tools that can be mounted to agricultural vehicles in a more practical way. However, this is far from an optimal solution. Although these types of basic tractor mounted lifting tools look more practical, disadvantages, such as difficulties in operation/control, mechanical failures and component breakage during operational use due to design errors, low levels of lifting capacity, insufficient ergonomics, etc., lead users to seek more convenient tools. These disadvantages can be eliminated by a lifting tool which is designed using advanced design, engineering and optimisation techniques with consideration due to the user-defined needs and specification.

This paper describes a CAD/CAE and structural optimisation-based total design algorithm which was put into practice in a real case study. The following sections of the paper introduce the steps of the algorithm in detail in terms of a case study for design and structural optimisation of a tractor mounted telescopic boom crane.

2 Materials and methods

2.1 Application algorithm

The research presented a computer-aided structural optimisation algorithm which can be implemented for the total design, development and improvement of agricultural machinery in detail. The algorithm has been developed based on advanced CAD/CAE technologies and structural optimisation techniques. This algorithm is represented by the flow chart, as shown in Fig. 1. In the chart, the procedures begin with the design decision, needs and definition of the constraints and then continue in the digital environment with a practical virtual design strategy. Following the virtual design, optimisation and evaluation steps, the subsequent application procedures are completed with physical prototyping, experimental design validation and manufacturing drawing procedures.

2.2 Case study: tractor mounted telescopic boom crane

The algorithm has been put in practice utilising CAD, numerical and experimental techniques in an industrially focussed and applied case study. In the case study, it is focussed on designing a tractor mounted telescopic boom crane (TMTBC) for small- and medium-sized agricultural enterprises. Following interviews conducted with growers, field observations and investigations on existing lifting and transportation tools, the design features and constraints were defined. Some of the major design features are given in Table 1.

2.3 Material selection and testing

The crane's operating condition, maximum loading capacity and possible manufacturing techniques were considered for the material selection procedures of the crane's design and as such, it was decided to manufacture the crane as a steel construction. For the strength analysis and structural optimisation procedures, which take place in the following steps of the algorithm, the yield strength point of the material has been defined as a failure criterion. This failure criterion and other experimentally determined material properties have critical importance for finite-element method (FEM)-based simulations, optimisation and total design evaluation progression. Therefore, to obtain the required mechanical properties of the materials, several specimens were collected randomly from the steel material-based sheet metal which were chosen for the production of the crane, with different thicknesses, and then tensile and fatigue tests were utilised. Details of material testing progress and the test results are presented in Fig. 2.

2.3.1 Tensile testing

In the tensile testing procedure, a 100 kN capacity SHIMADZU AG–X was utilised, and the standards for metal materials (TS EN ISO 6892-1) were followed. Three different thickness rectangular specimens (2.5, 6, and 8 mm) were prepared using water–jet cutting technology in accordance with the dimensions given in the standards. Nine specimens were tested in total. The specimens were randomly extracted from sheet metal raw materials which were used for the carane's prototype manufacturing. All data obtained from the tests were re-ordered, and average values of 280.26 $\pm$ 8.94, 404.23 $\pm$ 1.14 and 348.69 $\pm$ 11.36 MPa were calculated for yield, tensile and fracture points of the material, respectively.

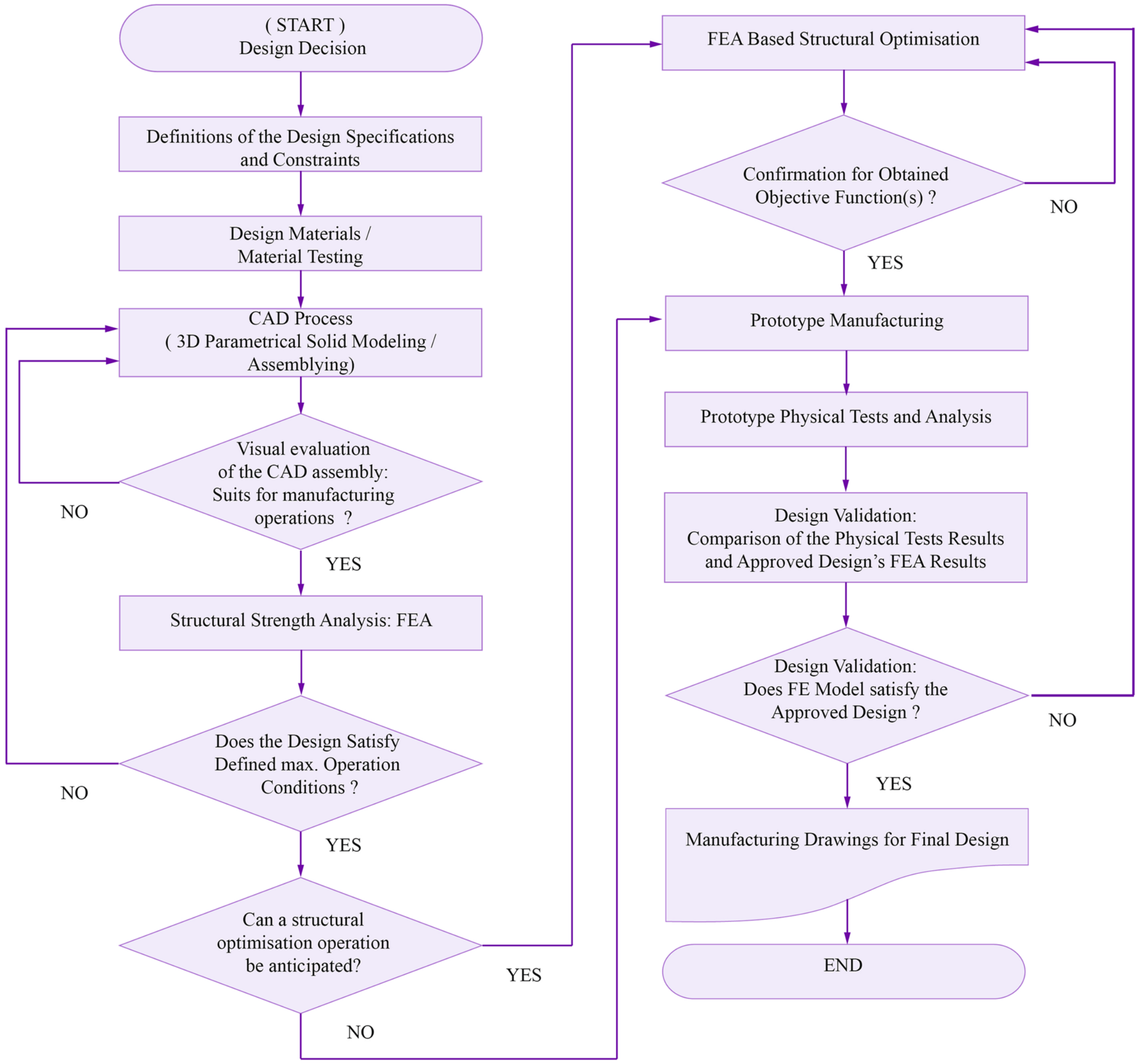

Fig. 1 Flowchart representation of the application algorithm

Table 1 Some of the design features of TMTBC

Max safe loading capacity	<700 kg
Max. boom openning length	2.5 m
Max lifting height. (Static condition with lifting angle of 45°)	3 m
Total rotation ability (right and left sides)	180 [°]
Crane motion control	The tractor hydraulic system
Boom characteristic	Telescopic (2 components)
Tractor connection	The tractor three-point linkage (portable)

2.4 Fatigue testing

To evaluate the operating life of the crane's components in defined loading conditions, fatigue testing was undertaken. The fatigue testing was conducted for five identical cylindrical specimens which were taken randomly from the crane's construction steel materials. A Rotating Beam Fatigue Testing System (ISO 1143: 2010/TS ISO 1143) was utilised for testing. The tests were conducted on the selected specimens under different dynamic loading conditions. All the data obtained from the tests were evaluated according to Wohler strategy and are represented in Fig. 2. The infinite life cycle (approximate cycle of 10^7) was obtained at a stress magnitude of 197 MPa.

3 3D solid modelling

Engineering calculations, manufacturing limitations, design features and constraints were considered for each single part of the design process, and then every single component

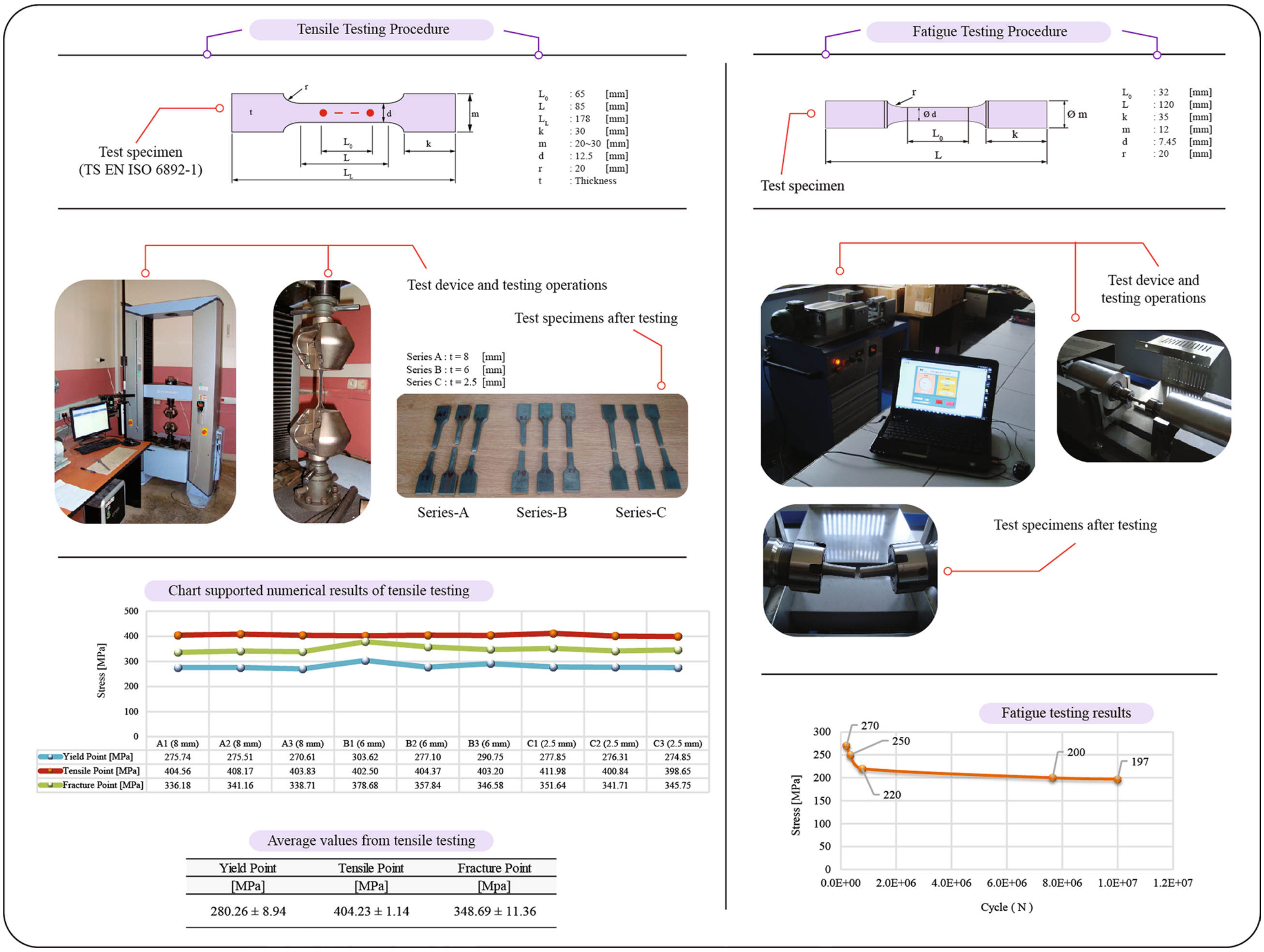

Fig. 2 Material tests

of the crane was modelled using the SolidWorks 3D parametric solid modelling design software. Subsequently, all components were assembled into an assembly module of the software considering the crane's real-life operating conditions. The digital prototype of the crane has motion ability, as it would have in real-life operating conditions. Steel-based materials were defined for nearly all of the components of the crane during the modelling operation. At the end of the digital prototyping procedure, the total mass of the crane construction was calculated as 394 kg, which upon evaluation is an acceptable mass within the design constraints. Statistical information, modelling progress and tractor mounting of the crane's CAD model are shown in Fig. 3.

Motion of the crane is provided by three hydraulic cylinders which can be controlled through the tractors hydraulic system unit with a joystick. The crane's maximum safe loading magnitude was set as 700 kg. This magnitude would affect the crane the most when the telescopic boom is positioned fully opened and parallel to the ground. Therefore, the calculations were conducted for this position of the boom as the worst-case loading scenario. Properties belonging to the hydraulic cylinders and maximum loading scenario are presented in Fig. 4.

The crane is evaluated in the virtual environment considering criteria, such as interaction, collision and unison between components, rotary motion and control ability, maximum lifting angles and boom opening/closing locations, degree of freedom for moving parts, manufacturability, etc. As a result of the evaluations carried out on the crane to assess the manufacture of a physical prototype, no negative aspects were encountered, so the next step of the algorithm for the FEM-based structural stress analysis was initiated.

3.1 FEM-based stress analysis

In the FEM-based stress analysis, it is possible to investigate failure cases of the crane's structural components at the worst loading scenario. Failure is defined as permanent

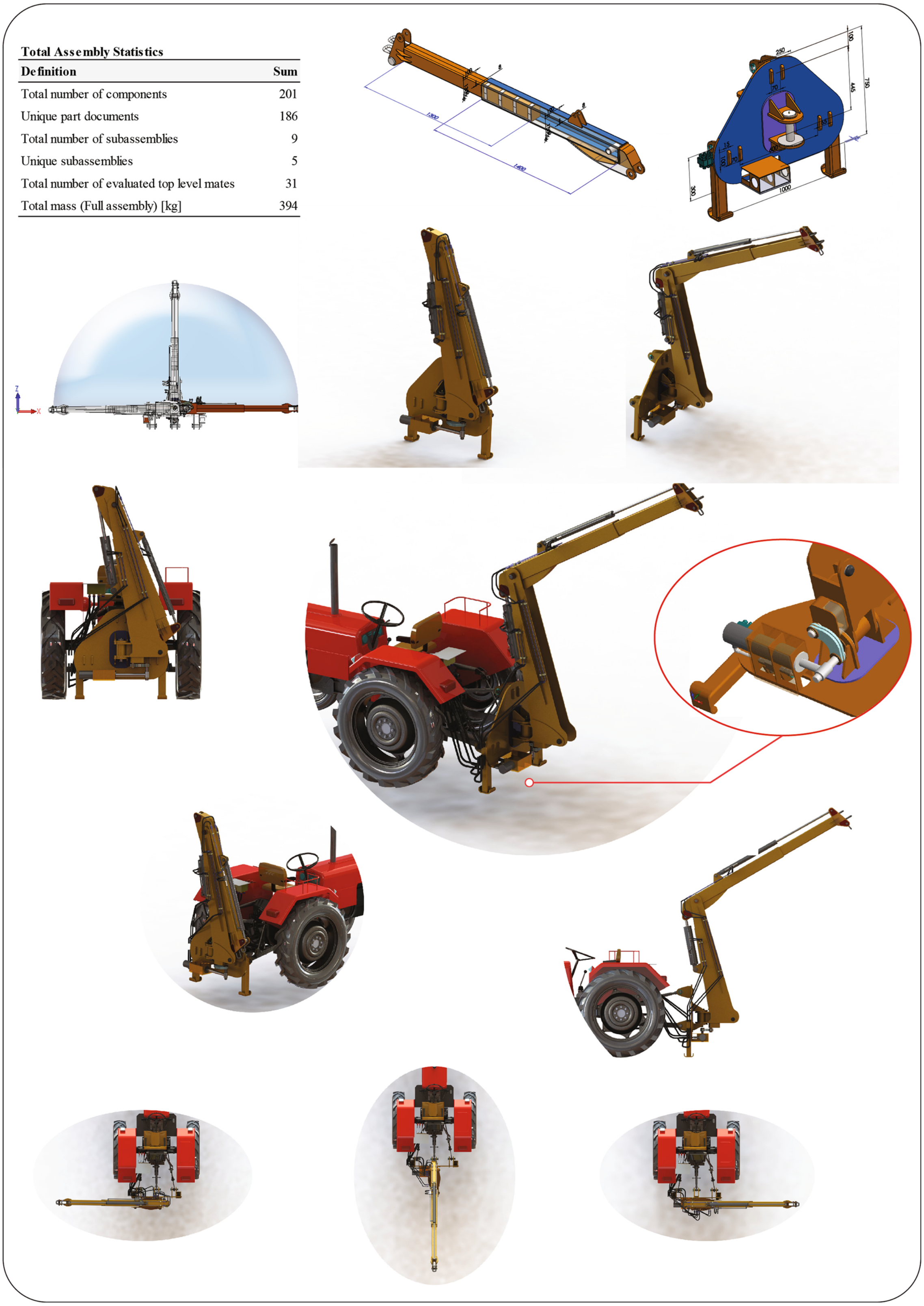

Total Assembly Statistics

Definition	Sum
Total number of components	201
Unique part documents	186
Total number of subassemblies	9
Unique subassemblies	5
Total number of evaluated top level mates	31
Total mass (Full assembly) [kg]	394

Fig. 3 Solid modelling

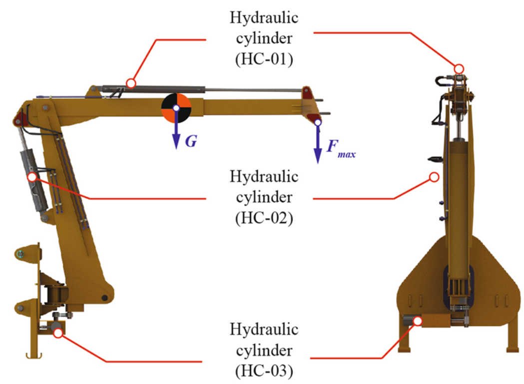

Properties of hydraulic cylinder-piston sytems

Hydraulic cylinder	Stroke [mm]	Lenght of piston rod [mm]	Dia. of piston rod [mm]	Inner dia. of cylinder [mm]	Outer dia. of cylinder [mm]
HC-01	700	930	25	50	60
HC-02	400	600	32	90	105
HC-03	270	425	30	80	90
Piston course time: 8 [s]					

Fig. 4 Hydraulic cylinder-piston systems

deformation or instant breaking on the structure when it is loaded beyond its constituent material's elastic limit [7]. Ductile steel-based materials are defined for the majority of the crane's components. The failure case is seen in two steps in these types of ductile materials, as explained by the Hookes law [8]. Approaching the yield point of the material, the first failure occurs which is known as plastic deformation. With an increase in loading, subsequent breaking may occur if the load exceeds the fracture point of the material. The failure evaluation was conducted by making a comparison between the material yield point and the Von Misses stress magnitudes extracted from the finite-element analysis (FEA) on the crane's components. FEA was set up considering static loading, bonded contact, and linear and isotropic material model assumptions. The analysis was conducted using SolidWorks simulation commercial finite-element code. Meshing operations were carried out using the meshing functions of the FE code [9]. In the meshed structure, 10 nodes second-order parabolic solid element type was used, and a total of 585,904 nodes and a total of 331,344 elements were obtained. The FE model had a total of 1,740,303 degree of freedom (Fig. 5). The critical material properties, such as yield, tensile and fracture strength points used in the FEA, were obtained from the tensile tests (Fig. 2). In addition to these properties, elastic modulus of 210 GPa, poisson's ratio of 0.3 and density of 7850 kg m^{-3} were defined in the FEA.

After running the FEA process, deformation and stress distributions were obtained for the crane's components for the pre-described worst-case scenario. In the FEA post-processing step, output screens were displayed, which detailed the maximum deformation and the maximum equivalent stress (Von Mises) distribution occurring on the crane construction (Fig. 6).

The simulation output extracted the maximum displacement of 20.544 mm at the loading point of the boom in the direction of vertical loading. The displacement evaluation showed that this magnitude was in the acceptable limits of the design constraints and would not adversely affect the crane's operation. In addition to this, to see clear visual failure information locally and globally, stress distributions on the crane components were evaluated according to the factor of safety (FOS) which shows the Von Mises stress ratio according to the yield strength of the component materials. As a result of the general FEA evaluation, the simulation outputs do not indicate any significant failure on the crane components and it is concluded that the crane design is durable enough under the defined maximum loading conditions.

However, as the overall design assembly has been evaluated as durable, it does not mean that the individual components of crane are of the best design. Most especially in this context, one of the crane's most critical elements which has moving parts and works under high loading condition is the telescopic boom. Therefore, it is quite important to have an optimised structure for the boom components. This importance led the study to make a detailed investigation of the stress distribution on the boom component and consider structural optimisation. To do this, a detailed FEA was established specifically for the boom components. ANSYS Workbench Multi-Physics FE code was utilised for

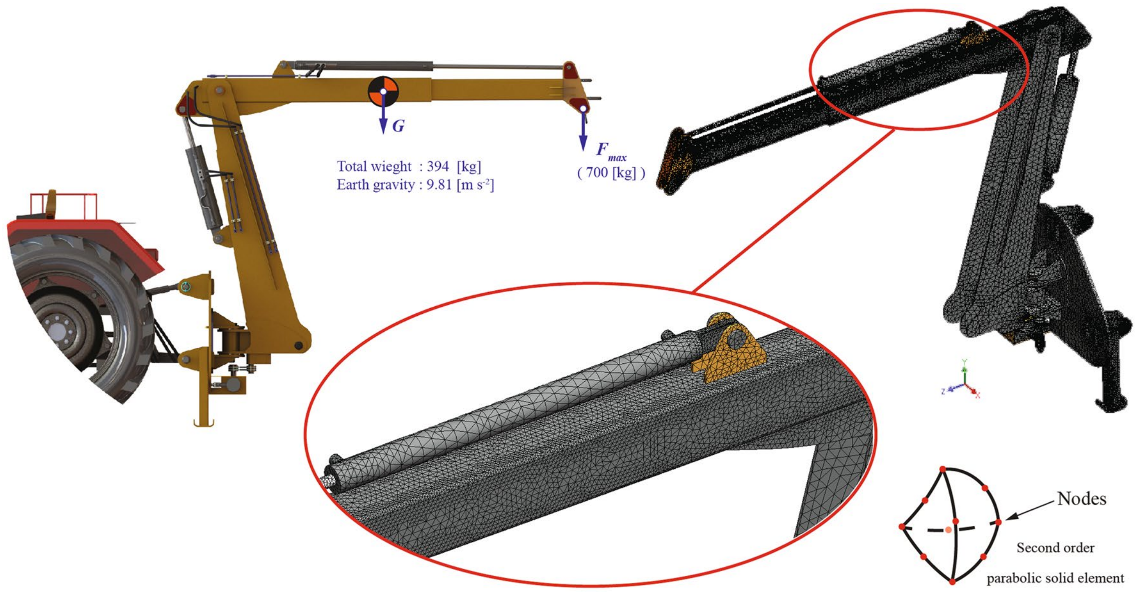

Fig. 5 Loading position and mesh structure

the detailed FEA procedure. Identical boundary conditions and material properties which were defined for the previous global FEA study were used for this detailed FEA. Structural meshing functions were used in the software [10]. The FE model was described by a total of 53,719 elements and a total of 210,131 nodes (Fig. 7).

The details of the equivalent stress distribution on the boom components were obtained from the FEA solution. The FEA output plots did not highlight any point on the boom, where it would exceed the materials failure criteria (270 MPa). The maximum equivalent stress was 192.59 MPa at the boom-tower connection interface (Fig. 8). This maximum stress point was at the local zone on the boom, where the moment force is at its maximum. This point has a sharp corner welding line. Therefore, although there is a relatively higher stress value obtained at that point, the other regions showed that the values of stress were quite lower than the materials failure criteria for the components. This information led the study to consider a structural optimisation setup on the boom-tower connection components to gain optimal geometric parameters of the components with the aim of reducing the material mass within the acceptable stress load. The FEA output plots of the detailed stress distribution on the boom and boom-tower connection components are shown in Fig. 8.

3.2 Structural optimisation of boom-tower connection components

An optimisation study can be described with three features: design variables (parameters), design constraints (limits/bounds) and objective function [11–13]. The aim is to ascertain the best parameters depending on the objective function and the constraints. The optimisation study in this paper was set up in the DesignXplorer module of ANSYS Workbench commercial FEA code. DesignXplorer (DX) is an optimisation module which searches for the optimum design parameters according to the design constraints and objective function by referencing to response parameters obtained from pre-solved FEAs. The module uses a design of experiments (DOE) approach in searching for the optimum design parameters. DOE is a technique used to determine the location of sampling points and is included as part of the response surface, goal driven optimisation and six sigma analysis systems [14]. Design variables used in this study are selected according to the geometric features of the components, and four of the design variables were utilised in defining the study for two connection components (Fig. 9). Response parameters were defined as equivalent stress and material mass, and the objective function of the study was defined as minimising material mass.

According to the defined parameters and boundary definitions given in Fig. 9, the module created 25 automatic design sets to be solved. After the solving procedure, numerical results were obtained, and 3D surface charts were utilised to observe the changes visually between input and response parameters. Some of the output charts are given in Fig. 10.

Accordingly, the increase of P1 and P2 provides an increase for the variable mass value of component-01; however, in this case, the global maximum equivalent stress values are decreasing. Similarly, the increase of P3

Fig. 6 FEA evaluation

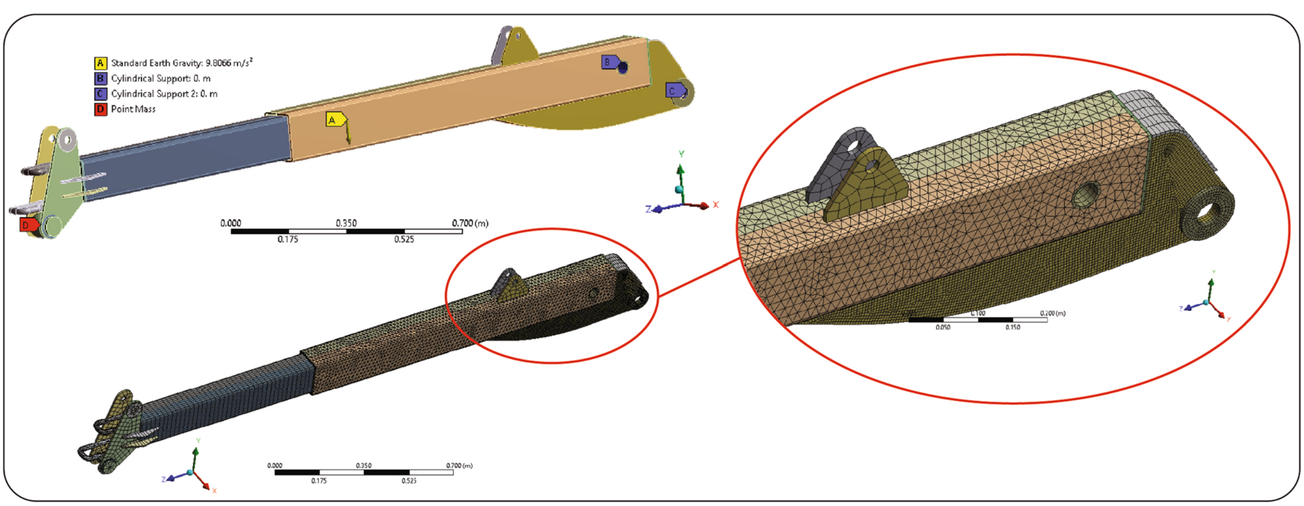

Fig. 7 Boundary condition and mesh structure of the telescopic boom

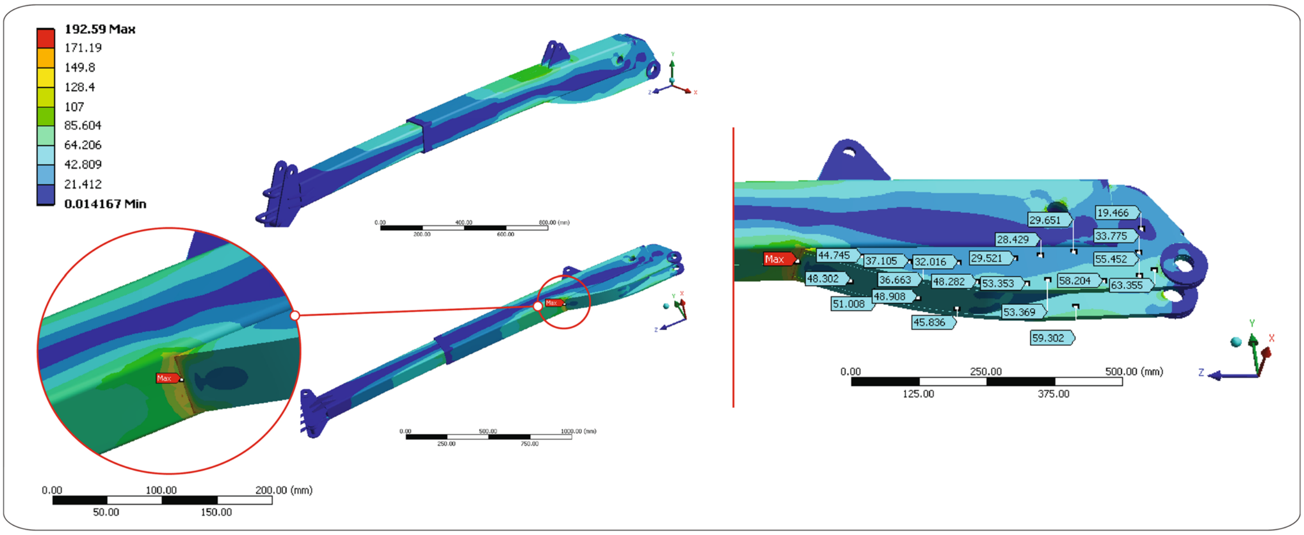

Fig. 8 Equivalent stress distribution on the boom and boom-tower connection components

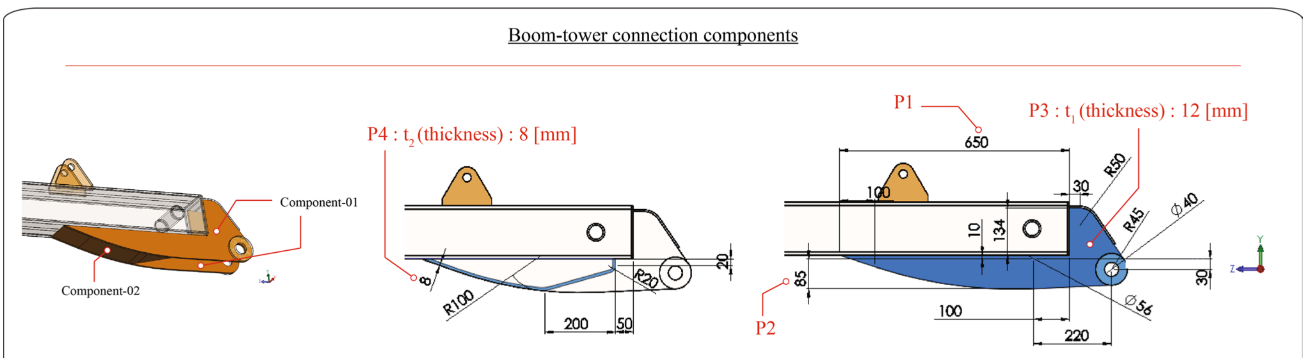

Design variables and variable limits

Component No		Component-01			Component-02
Variable Code		P1	P2	P3	P4
Initial Design Variables	[mm]	650	85	12	8
Variable Limits	[mm]	400 ≤ P1 ≤ 900	70 ≤ P2 ≤ 110	6 ≤ P3 ≤ 20	4 ≤ P4 ≤ 16

Fig. 9 Selected geometrical design variables

and P4 provides an increase in total boom mass. However, global maximum equivalent stress values show an increase in relation to the increase of P3, whilst there is no significant change seen in the stress value in relation to changes of P4. After this observation, the next step is to find out the best design parameters for the objective function of defining the optimum mass. To enable this, the goal driven optimisation (GDO) approach is utilised in the DX module. In the approach, and in consideration of the design boundaries and the objective importance, several candidate design sets were extracted from pre-solved response surfaces (Fig. 10) and selected one of them as the best design set. According to the desired objectives and design boundaries defined in Tables 2 and 3, the three best matched design sets were rated (Table 4). In this rating evaluation process, it was seen that the candidate-01 could provide a better match to the desired objectives which could provide a minimum mass/component thickness with acceptable stress magnitudes (under failure criteria). Therefore, candidate-01 was selected as the best design set. Table 5 presents the comparison of the initial design parameters and candidate-01 design set parameters. This comparison states that, although stress magnitudes on related components are increased, they are within acceptable limits which

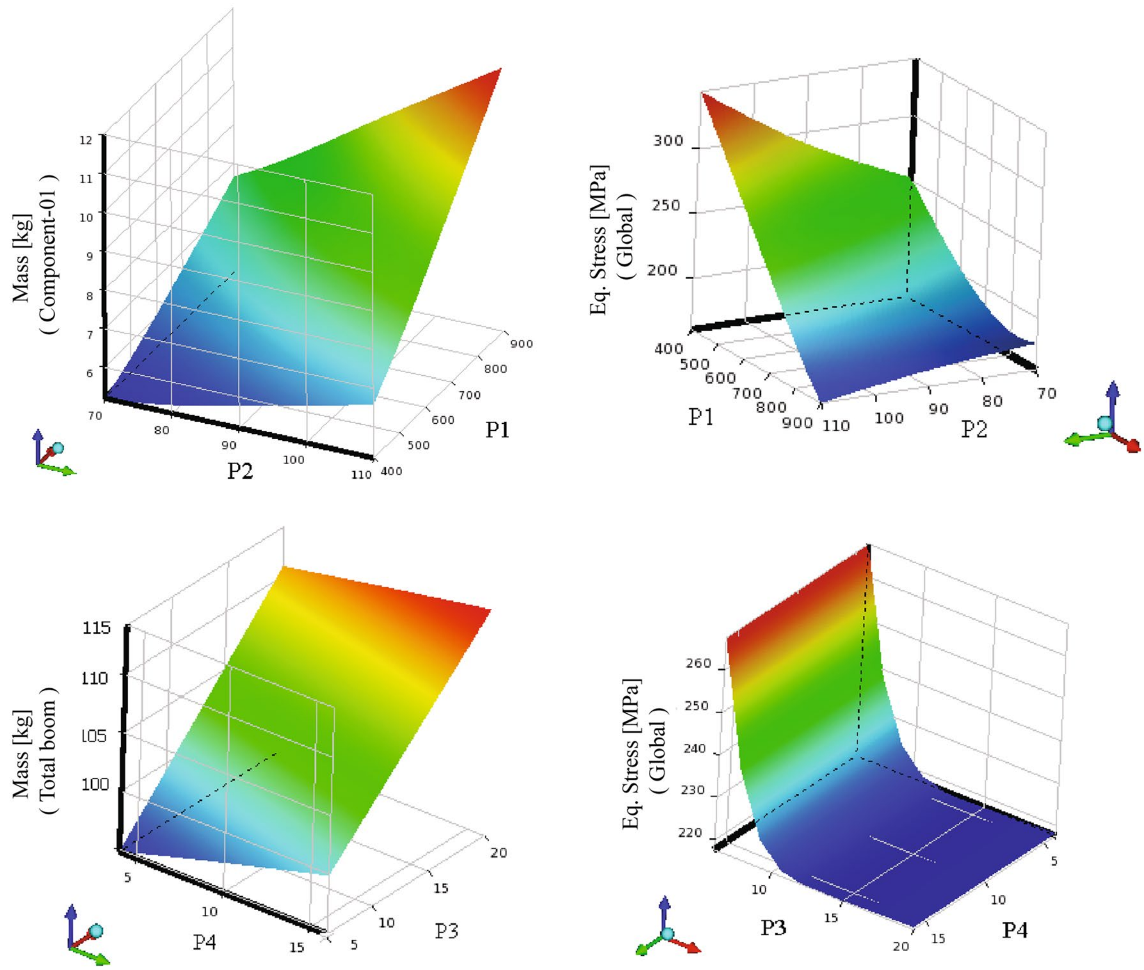

Fig. 10 Variation of response parameters (equivalent stress and mass) against input parameters (P1, P2, P3, P4)

Table 2 Desired definition of design parameters in GDO approach

Design variables	Lower bound (mm)	Upper bound (mm)	Certain bound (mm)	Objective	Objective importance
GDO—definitioin of design variibles					
PI	400	900	–	–	Default
P2	70	110	–	Minimize	Higher
P3	6	20	–	Minimize	Higher
P4	4	16	–	Minimize	Higher

Table 3 Desired definition of response parameters in GDO approach

Response variables	Unit	Specific target	Objective	Objective importance
GDO—definition of response paramters				
Max Eq. stress (component-01)	[Mpa]	–	≤260	Higher
Max Eq. stress (component-02)	[Mpa]	_	≤260	Higher
Max Eq. stress (boom/ gobal)	[Mpa]	–	≤260	Higher
Mass (component-01)	[kg]	–	Minimize	Higher
Mass (component-02)	[kg]	–	Minimize	Higher
Mass (boom/ bobal)	[kg]	–	Minimize	Higher

Table 4 Best matched three design sets extracted from GDO approach

Candidate design sets	PI (mm)	P2 (mm)	P3 (mm)	P4 (mm)	Max. Eq. stress (comp.-01) (MPa)	Max. Eq. stress (comp.-02) (MPa)	Max. Eq. stress (boom/global) (MPa)	Max. Eq. stress (comp.-01) (kg)	Max. Eq. stress (comp.-02) (kg)	Mass (boom/global) (kg)
GDO—rating of Candidate designs sets										
Candidate-01	550.250	78.223 **	7.927 **	4.226 ***	215.170 ***	215.390 ***	242.680 ***	3.776 ***	1.600 ***	100.500 ***
Candidate-02	625.250	80.567 –	7.351 *	4.351 ***	216.430 ***	199.710 ***	243.080 ***	3.850 **	1.650 ***	100.440 ***
Candidate-03	760.250	71.778 ***	7.543 **	6.217 **	200.510 ***	153.620 ***	239.180 ***	4.065 **	2.340 **	101.440 **

are kept under the failure criteria. When objective function (minimising mass) is considered, the comparison table also states that there is a reduction in material mass. These are calculated as 43.976 % (2.964 kg), 46.667 % (1.4 kg) and 5.916 % (6.320 kg) for component-01, component-02 and total boom mass, respectively.

As a result of the total optimisation study, the candidate 01 design set has been approved as the optimum design set. In the subsequent manufacturing process, the standard thicknesses of sheet metals are considered. Therefore, optimised design parameters have been converted to the nearest integer values, and then, these parameters have been updated in the virtual prototype of the crane's boom in the CAD software. Updated design parameters are given in Table 6.

3.3 Fatigue life evaluation for the crane components

Fatigue life evaluation studies are common, most especially for machine elements, such as gears, axles, pulleys, etc., which operate under high cycle repeated loads [15–18]. Although the crane meets with a relatively high magnitude load, its operating condition is not in this class of high cycle repeated loads as much as the rotary machine elements. Therefore, no likely failure case is predicted as a cause of high cycle fatigue on the crane components within their economic life. However, as a fatigue failure case is not predicted, a safe operating life prediction can be made for the crane components. In the previous section discussing the fatigue test, the results showed that the life cycle of the crane's material was at the stress limit of 197 MPa. The optimised structure of the crane has a maximum stress magnitude of 242.680 MPa under the worst loading scenario. This maximum stress magnitude on the optimised structure occurs after approximately 400,000 loading cycles (Fig. 2). If it is assumed that the crane would be operational for eight hours per day and loaded/unloaded 20 times per hour, hence 160 cycles per day. Using this assumption, the crane could be operated without any risk of fatigue failure for $400{,}000/160 = 2500$ working days or $2500 \times 8 = 20{,}000$ working hours. The most common agricultural machine is the tractor which is typically employed in agricultural fields. The average economic life for a tractor based on international standards is quoted as 1000 working hours per year [19]. In addition, some researchers quote that typical working hours per year for a hydraulic lifting apparatus is in the range of between 25 and 300 working hours [20]. In short, such information leads this study to conclude that the crane structure could be operated without any fatigue failure during its economic life.

3.4 Manufacturing of the physical prototype

Following the design optimisation process, 2D manufacturing drawings are prepared in the CAD software for each

Table 5 Comparison table of optimised parameters

Parameters	P1 (mm)	P2 (mm)	P3 (mm)	P4 (mm)	Max. Eq. stress (comp.-0l) (MPa)	Max. Eq. stress (comp.-02) (MPa)	Max Eq. stress (boom/global) (MPa)	Mass (c (kg)	Mass (comp.-0l) (kg)	Mass (boom/global) (kg)
GDO—comparison of initial design parameters and selected candidate design set										
Initial value	650	85	12	8	184.760	192.590	192.590	6.740	3	106.820
Optimised value	550.250	78.223	7.927	4.226	215.170	215.390	242.680	3.776	1.600	100.500
Variation (%)	15.346 (−)	7.973 (−)	33.942 (−)	47.175 (−)	16.459 (+)	11.839 (+)	26.009 (+)	43.976 (−)	46.667 (−)	5.916 (−)

(+) ıncrease (−) decrease

Table 6 Final design parameters

Component no	Component-01			Component-02
Variable code	P1	P2	P3	P4
GDO—updated design parameters				
Initial values (mm)	650	85	12	8
Updated values (mm)	550	78	8	5

of the crane's components, and the physical prototype of the crane was produced according to these drawings part by part using appropriate manufacturing techniques. The manufacturing operation was conducted by a commercial agricultural machinery enterprise in Antalya, Turkey. Some visuals from manufacturing process and the physical tractor connection are shown in Fig. 11.

3.5 Physical test and FEA validation

The manufactured prototype was tested physically to evaluate its real-life operating and deformation behaviour under a pre-defined loading scenario. In parallel, an FEA validation was carried out by performing a comparison of the experimental and FEA structural stress data. First, a physical investigation was conducted visually. The prototype was operated under the maximum load of 700 kg over several of the booms positions to observe total functionality and unpredictable, undesired behaviour at the boom openings, lifting angles whilst rotating, interaction and synchronism between components, etc. No negative behaviour is witnessed from this visual observation. An experimental stress analysis was then carried out on the critical components of the crane—the boom and boom-tower connection components—utilising a strain-gauge (SG) technique.

HBM/KR-Y series, 0°/45°/90°, 120 Ω, three element rosette strain gauges with HBM/QuantumX 840A model, 8 channels, 24 bit resolution capacity universal data acquisition module, a ZEMIC/H3-C3-13/5.0t-B6 model, 50 kN capacity S-type load cell with computer-aided measurement and data visualising systems were utilised in the experimental study [21, 22]. Stress measurements were carried out simultaneously with the loading operation which was prepared in accordance with the worst loading scenario. Each of the measurements was recorded with a 50 Hz sample rate for 30 s, and the operation for each was repeated three times under identical conditions. Placement of the strain-gauge rosettes and experimental setup are shown in Figs. 12 and 13, respectively.

4 Results and discussions

According to the physical tests carried out on the crane, no negative and/or signs of failure were observed visually. The physical deformation behaviour of the crane was in agreement with the simulation in the virtual environment (Fig. 6). The experimental stress results which were obtained from critical components on the crane also proved that the crane was durable and stable under the worst loading scenario. At no point was the material's failure criteria exceeded. The experiment found that the maximum equivalent stress was 133.09 MPa and minimum equivalent stress was 16.51 MPa at the locations of SG-05 and SG-04, respectively. The experimental results for equivalent stress at the SG locations are given in Table 7.

In developing the overall design algorithm for the crane, the virtual and physical tests are utilised successfully. However, as simulations provide a significant contribution to the design process, it is important to determine the approximate level of the simulations in accordance with the physical conditions to approve the final design decisions. To enable this, relative error percentages were calculated between the experimental and FEA results [23]. A comparison of the numerical results is shown in Fig. 14.

According to the chart presented in Fig. 14, this comparison showed that there was a good correlation between the experimental and FEA results. The maximum error was

Fig. 11 Manufacturing process and tractor connection of the prototype crane

15.75 % and the minimum error was 4.87 % at the measurement points SG-05 and SG-02, respectively. The average error of all points was calculated as 9.53 %. In fact, the differences between the physical and FEA conditions can be attributed to virtual and physical errors, such as geometric errors in CAD models, FE models (meshing structure) described in FEA, assembly/mismatch/material errors in physical structures and human factors in experiments. Similar research found in the literature showed that a good FEA setup could come up with maximum errors of 10–15 % relative to physical conditions, and there were inevitable errors between the experiment and the FEA simulations which can reach errors of 20–30 % depending on simulation complexity [24–27].

5 Summary and conclusions

In this research, an individual advanced computer-aided design and engineering application-based total design algorithm are introduced, and this algorithm has been put into practice in a case study successfully. The details of the study, numerical and experimental methods have been utilised and virtual prototyping applications validated experimentally. The case study presented in this paper is concluded with a successful product prototype which is ready for manufacturing. The virtual applications helped to reduce the number of design iterations and procedures, such as redesign of parts, repeating experimental tests and physical part manufacturing. One of the significant points here was that the first prototype was validated experimentally and appointed as the final design. This contributed positively to efficiency of the design, working time, design and manufacturing costs etc.

Manufacturing of the physical prototype and experiments has been carried out in a local agricultural machinery manufacturer's workshop in Antalya, Turkey. In the context of industry-university collaboration, the application of the methodology has contributed to industry in having the original optimal design strategy. This strategy resulted in a product that can also contribute to similar small- and medium-sized agricultural enterprises and agricultural machinery manufacturers. The infrastructure and facilities utilised through this research and development methodology are also applicable for the design and optimisation of several types of equipment/machinery used in agricultural production, such as soil tillage tools, planting machinery, harvesters, etc. Although there is an increase, it is true to say that the usage of these advanced CAD/CAE and structural optimisation technologies in the agricultural machinery design field is still limited. Therefore, this study provides a unique CAD/CAE and experimentally driven total

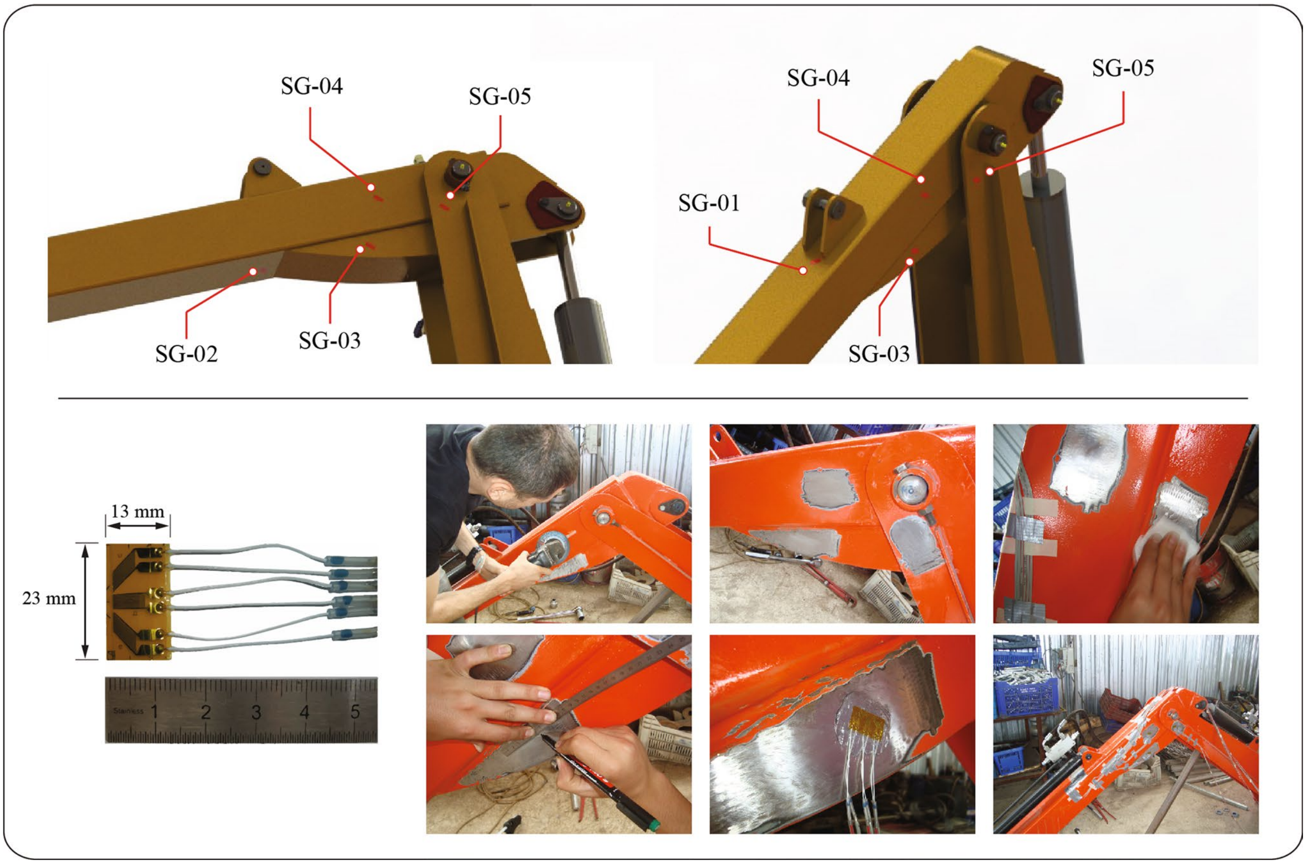

Fig. 12 Strain-gauge placement process

Fig. 13 Experimental setup

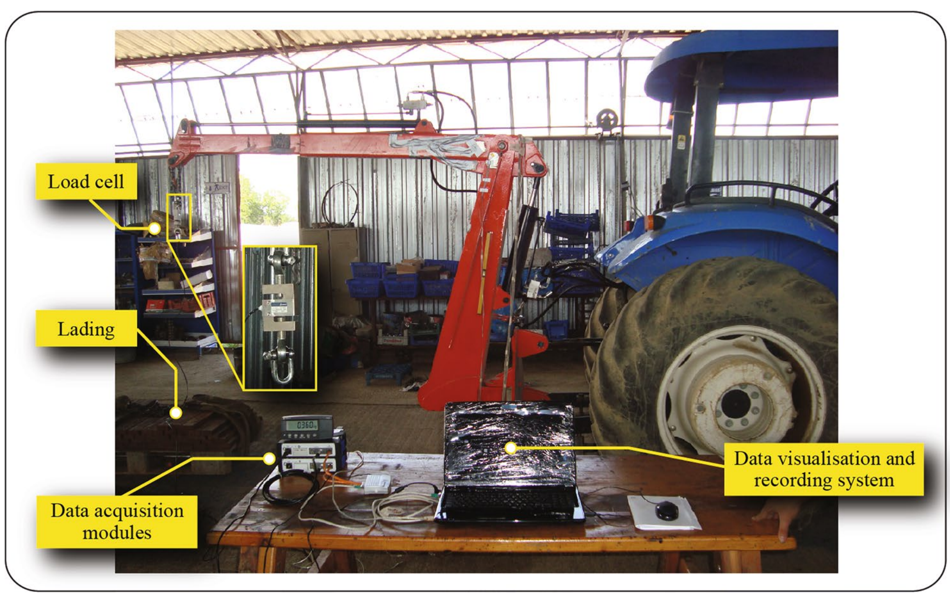

Table 7 Experimental stress measurement results

Strain-gauge location	Parameters	Record-01 (MPa)	Record-02 (MPa)	Record-03 (MPa)	Averages of the records (MPa)	Standard deviation [±]
Results of the experiinental stress measurement						
SG-01	Eq. stress (MPa)	73.58	73.62	73.63	73.61	0.02
SG-02	Eq. stress (MPa)	96.33	96.22	96.19	96.24	0.08
SG-03	Eq. stress (MPa)	36.71	36.83	36.91	36.82	0.10
SG-04	Eq. stress (MPa)	16.43	16.54	16.55	16.51	0.06
SG-05	Eq. stress (MPa)	133.37	132.93	132.96	133.09	0.25

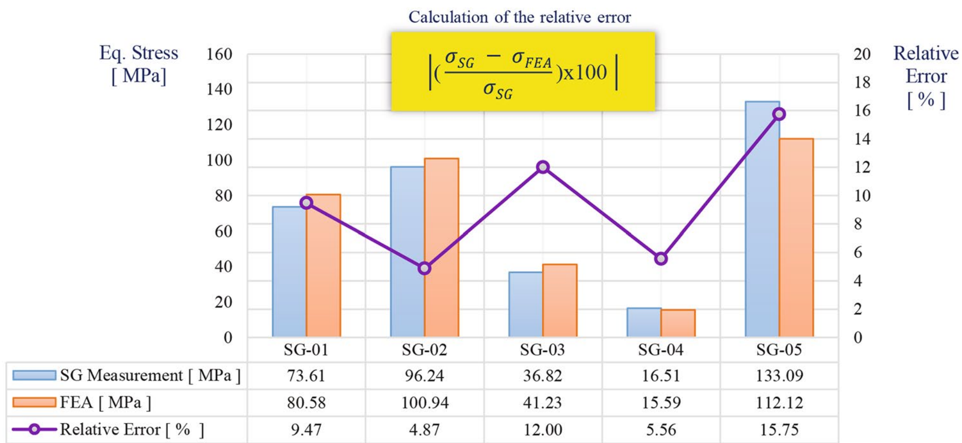

Fig. 14 Chart comparison of the stress results

design pathway for similar products, which contributes to further research into the utilisation of engineering simulation technology for agricultural machinery design, analysis and related manufacturing subjects.

Acknowledgments This study was funded by the Scientific Research Project Coordination Unit, Akdeniz University (Project No: 2011.01.0104.006).

References

1. Ogot M, Kremer G (2004) Engineering design: a practical guide. Trafford Publishing 1412038502:432
2. Haik Y, Shahin T (2010) Engineering design process. 2nd Ed. Cengage Learning, ISBN: 9780495668145
3. Childs P (2004) Mechanical design. Elsevier Butterworth-Heinemann Publications. 2nd Ed., ISBN: 0750657715
4. Rembold U, Nnaji BO, Storr A (1994) Computer integrated manufacturing and engineering. Addison Wesley Publication. ISBN 0201565412:664
5. Topakci M, Celik HK, Canakci M, Rennie AEW, Akinci I, KarayeL D (2010) Deep tillage tool optimization by means of finite element method: case study for a subsoiler tine. J Food Agric Environ 8(2):531–536
6. Celik HK, Lupeanu ME, Rennie AEW, Neagu C, Akinci I (2013) Product re-design using advanced engineering applications and function analysis: a case study for greenhouse clips. J Braz Soc Mech Sci Eng 35:305–318
7. Risitano A (2010) Mechanical design. CRC Press 9781439811696(2011):650p
8. Ugural AC, Fenster SK (2003) Advanced strength and applied elasticity. 4th Ed. Prentice Hall, ISBN: 0130473928
9. Solidworks (SW) Software Product (2014) Online help documentation: Meshing. Dassault Systèmes. Available http://help.solidworks.com/2014/english/solidworks/cworks/c_background_on_meshing.htm?id=96bc9cfddf7e453ebc35e86a44b39c6b#pg0. Accessed 12.10.2014
10. ANSYS Software Product (2013) Overview of the meshing process in ANSYS Workbench. Release Documentation for ANSYS Workbench. ANSYS Inc, USA
11. Christensen PW, Klarbring A (2009) An introduction to structural optimization. Springer. ISBN 9781402086656:211p
12. Rao SS (2009) Engineering optimization—theory and practice. 4th Ed. Wiley. ISBN: 9780470183526
13. Deb K (2004) Optimization for engineering design: algorithms and examples. Prentice Hall Publication. ISBN 9788120309432:396
14. DesignXplorer (DX) (2013) ANSYS DesignXplorer: Design exploration user's guide Release 15.0, Release Documentation for ANSYS Workbench, ANSYS Inc., USA
15. Gülec S, Aran A (1983) Fatigue strength of steel and cast iron. TUBITAK Marmara Scientific and Industrial Research Institute Publication, Gebze/Istanbul, Turkey. **(in Turkish)**
16. Bannantine JA, Comer JJ, Handrock JL (1989) Fundamentals of metal fatigue analysis. Prentice Hall, USA. ISBN 978-0133401912
17. Stephens RI, Stephens RR, Fuchs HO (2001) Metal fatigue in engineering, 2nd edn. Wiley, USA. ISBN 978-0471510598

18. Nicholas T (2006) High cycle fatigue: a mechanics of materials perspective. Elsevier. ISBN: 9780080446912
19. TARMAKBIR (2014) Annual report of agricultural machinery sector in turkey. Turkish Agricultural Tool and Machinery Manufacturers Associations, P40, http://www.tarmakbir.org/haberler/tarmakbirsekrap2013.pdf. Accessed 08.09.2014
20. Ulger P (1972) Expenses of the Agricultural equipment and machinery and its calculation principles. Ataturk Univ J Faculty Agric 3(2):143–150 **(In Turkish)**
21. HBM (2011a) Datasheet: QuantumX Mx840a. Doc. No: B2924-2.0 En. Hottinger Baldwin Messtechnik Gmbh, Germany
22. HBM (2011b) Strain-gages and accessories. Doc. No: S 1265-1.0 En. Hottinger Baldwin Messtechnik Gmbh, Germany
23. Kurowski P, Szabo B (1997) How to find errors in finite element models. Machine Design 9:93–98
24. Celik HK, Caglayan N, Cinar R, Ucar M, Ersoy H. and Rennie AEW (2012) Stress analysis of a sample marine crane's boom under static loading condition. 5th International Mechanical Engineering Forum (IMEF2012), Prague, Czech Rep., ISBN: 9788021322912, pp 246–256
25. Caliskan K (2011) The optimisation of cab protective structure with finite element method (FEM) simulation verified with laboratory tests. Dissertation. Ege University, Turkey **(in Turkish)**
26. Degirmencioglu A (2003) Determination of stresses acting on a three-bottom moldboard plow under load. Scientific Research Project. Ege Üniversity, Project No: 98 Zrf 046. **(in Turkish)**
27. Krutz G, Thompson L, Claar P (1984) Design of agricultural machinery. Willey 047108672:473